Flagellar regeneration requires cytoplasmic microtubule depolymerization and kinesin-13

Liang Wang[1,*], Tian Piao[1,*], Muqing Cao[1], Tao Qin[2], Lei Huang[1], Haiteng Deng[1], Tonglin Mao[2] and Junmin Pan[1,‡]

[1]Protein Science Laboratory of the Ministry of Education, School of Life Sciences, Tsinghua University, Beijing 100084, China
[2]State Key Laboratory of Plant Physiology and Biochemistry, Department of Plant Sciences, College of Biological Sciences, China Agricultural University, Beijing 100193, China

*These authors contributed equally to this work
‡Author for correspondence (panjunmin@tsinghua.edu.cn)

Accepted 7 January 2013
Journal of Cell Science 126, 1531–1540

doi: 10.1242/jcs.124255

Summary

In ciliated cells, two types of microtubules can be categorized: cytoplasmic and axonemal. It has been shown that axonemal tubulins come from a 'cytoplasmic pool' during cilia regeneration. However, the identity and regulation of this 'pool' is not understood. Previously, we have shown that *Chlamydomonas* kinesin-13 (CrKin13) is phosphorylated during flagellar regeneration, and required for proper flagellar assembly. In the present study, we show that CrKin13 regulates depolymerization of cytoplasmic microtubules to control flagellar regeneration. After flagellar loss and before flagellar regeneration, cytoplasmic microtubules were quickly depolymerized, which was evidenced by the appearance of sparse and shorter microtubule arrays and increased free tubulins in the cell body. Knockdown of CrKin13 expression by RNA interference inhibited depolymerization of cytoplasmic microtubules and impaired flagellar regeneration. *In vitro* assay showed that CrKin13 possessed microtubule depolymerization activity. CrKin13 underwent phosphorylation during microtubule depolymerization, and phosphorylation induced targeting of CrKin13 to microtubules. The phosphorylation of CrKin13 occurred at residues S100, T469 and S522 as determined by mass spectrometry. Abrogation of CrKin13 phosphorylation at S100 but not at other residues by inducing point mutation prevented CrKin13 targeting to microtubules. We propose that CrKin13 depolymerizes cytoplasmic microtubules to provide tubulin precursors for flagellar regeneration.

Key words: Chlamydomonas, Cilia and flagella, Kinesin-13, Protein phosphorylation, Flagellar assembly

Introduction

Cilia and flagella (interchangeable terms) are evolutionarily conserved structures with presence from protists to human (Carvalho-Santos et al., 2011; Satir et al., 2008). Motile cilia and flagella provide cell motility as manifested in ciliates and sperm. In contrast, immotile cilia may harbor receptors or ion channels to control development and cell physiology (Christensen et al., 2007; Goetz and Anderson, 2010; Ishikawa and Marshall, 2011; Pazour and Witman, 2003). Cilia and flagella can be regenerated after amputation and, thus providing an excellent system to study cilia assembly (Lefebvre and Rosenbaum, 1986; Rosenbaum et al., 1969). Immediately after cilia amputation, cilia are rapidly assembled accompanying with instant synthesis of mRNA and proteins of the ciliary components, as has been shown in sea urchin embryo (Stephens, 1977), *Tetrahymena* (Guttman and Gorovsky, 1979) and *Chlamydomonas* (Baker et al., 1984; Lefebvre et al., 1980). During cilia assembly, ciliary components including tubulin dimmers are transported by Intraflagellar transport (IFT) from the cell body into cilia and incorporated into ciliary axoneme (Hao et al., 2011; Qin et al., 2004; Rosenbaum and Witman, 2002). Using pulse and/or pulse–chase experiments and inhibitor of protein synthesis, it has been concluded that there is a cytoplasmic pool of ciliary precursors including tubulins for cilia assembly (Guttman and Gorovsky, 1979; Remillard and Witman, 1982; Rosenbaum et al., 1969; Stephens, 1977). However, the identity and the regulation of this 'pool' of ciliary precursors are not known.

Tubulin is one of the major components of cilia. Changing microtubule dynamics has been shown to affect ciliogenesis and cilia length. In mammalian cells, modulating actin dynamics by pharmacological agents and protein kinase A activity results in increase of free tubulins and subsequent cilia elongation, though the mechanisms for the increase of free tubulins are unknown (Kim et al., 2010; Sharma et al., 2011). In *Tetrahymena*, katanin, a microtubule-severing protein (McNally and Vale, 1993), is required for cytoplasmic microtubule dynamics and cilia assembly (Sharma et al., 2007). Kinesin-13s are a class of microtubule depolymerizers and function in spindle dynamics to control chromosome segregation during mitosis as well as interphase microtubule dynamics (Ems-McClung and Walczak, 2010; Mennella et al., 2005). They have also been implicated in flagellar assembly and length control. Overexpression of a kinesin-13 homologue in *Leishmania*, which is localized along the length of the flagellum, results in shorter flagella whereas its depletion by RNA interference (RNAi) in *Trypanosome* leads to longer flagella (Blaineau et al., 2007). In *Giardia*, overexpression of a kinesin-13 rigor mutant S280N causes longer flagella and disrupts cytoplasmic microtubule dynamics (Dawson et al., 2007).

Chlamydomonas is a bi-flagellate eukaryote, widely used for studying cilia assembly and disassembly. In the absence of protein synthesis, flagella after amputation can be re-assembled to approximately half length (Rosenbaum et al., 1969; Weeks and Collis, 1976). How ciliary precursors including tubulins are 'activated' and become available for cilia assembly is not clear. Studies in *Ochromonas* show that cytoplasmic microtubules may play a role in flagellar regeneration (Brown and Bouck, 1973). Previously, we have shown that kinesin-13 in *Chlamydomonas* (CrKin13) undergoes protein phosphorylation and is involved in proper flagellar assembly (Piao et al., 2009). In this report, we characterized dynamic changes of cytoplasmic microtubules during flagellar regeneration and found that cytoplasmic microtubules were quickly depolymerized to provide tubulin precursors for flagellar assembly, which required CrKin13. CrKin13 is regulated by phosphorylation for its targeting to cytoplasmic microtubules. We hypothesized that cytoplasmic microtubules serve as a pool of tubulins for flagellar assembly and CrKin13 plays a key role in releasing this 'pool'.

Results

Inhibition of flagellar regeneration by taxol stabilization of microtubules and by reduction of CrKin13 expression

The assembly of axonemal microtubules requires not only microtubule dynamics per se but also cytoplasmic free tubulins. It is expected that tampering of microtubule dynamics would affect cilia assembly and elongation. In mammalian cells, treatment with taxol reduces cilia length whereas nocodazole treatment results in longer cilia, and changes of cilia length correlate with increase of cytoplasmic free tubulins (Sharma et al., 2011). In contrast, opposite phenotypes of flagella in *Giardia* are observed with these treatments (Dawson et al., 2007). To learn whether these drugs affect flagellar length in *Chlamydomonas*, steady state cells were treated for 4 h with taxol or nocodazole. No significant effects on flagellar length, however, were found (Fig. 1A). These data may reflect species or cell type specific response to these reagents.

Next, we examined whether perturbation of microtubule dynamics affected flagellar assembly during flagellar regeneration and flagellar elongation. LiCl treatment induces flagellar elongation in *Chlamydomonas* and in mammalian cells (Nakamura et al., 1987; Ou et al., 2009; Wilson and Lefebvre, 2004) and protein synthesis is not required (Wilson and Lefebvre, 2004). Indeed, 25 mM LiCl treatment induced flagellar elongation (Fig. 1B). Taxol treatment inhibited flagellar elongation induced by LiCl, indicating destabilizing cytoplasmic microtubules contributes to flagellar assembly, which is consistent with the observation in mammalian cells (Sharma et al., 2011).

We further examined the effect of taxol on flagellar regeneration. *Chlamydomonas* cells were deflagellated by pH shock, and allowed for flagellar regeneration. Cells assembled full length flagella around 2 h after deflagellation as shown previously (Rosenbaum et al., 1969) (Fig. 1C). When protein synthesis was inhibited by adding 10 μg/ml cycloheximide, flagella could be assembled but only to around half length, which was consistent with the view that protein synthesis and a cytoplasmic pool of flagellar precursors both contributed to the assembly of full length flagella in *Chlamydomonas* (Rosenbaum et al., 1969). When 40 μM taxol was present during flagellar regeneration, the initial rapid phase of flagellar assembly was greatly attenuated (Fig. 1C). Interestingly, taxol almost completely inhibited flagellar assembly in the absence of protein synthesis. The inhibitory effect of taxol on flagellar assembly can not be solely explained by its effects on axonemal microtubule dynamics since taxol alone still allowed assembly of almost full length flagella. It is likely that stabilization of cytoplasmic microtubules by taxol restricts the availability of tubulin precursors for flagellar assembly in the absence of protein synthesis.

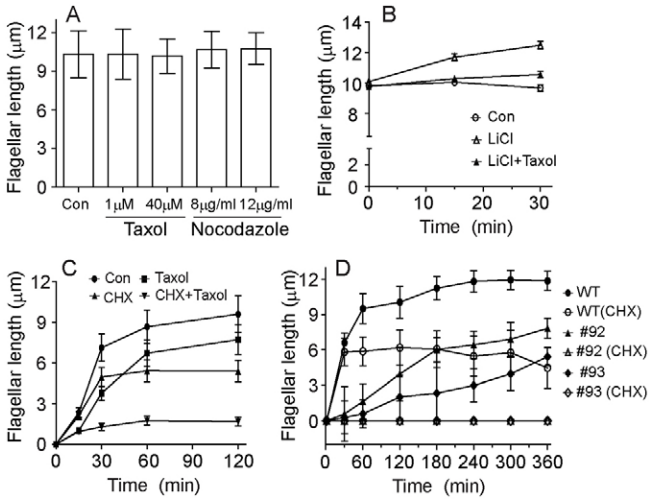

Fig. 1. Microtubule dynamics is required for flagellar assembly. (**A**) Effects of taxol and nocodazole on flagellar length of steady state cells. Steady cell cultures were treated for 4 h at the concentrations indicated followed by flagellar length measurement. Values in this and the subsequent figures are means±s.d. Con, control. (**B**) Inhibition of flagellar elongation by taxol. Steady state cells were induced for flagellar elongation by LiCl (25 mM) in the presence or absence of taxol (40 μM). (**C**) Inhibition of flagellar regeneration by taxol. Cells after deflagellation were allowed to regenerate flagella in the presence of taxol (40 μM) and/or cycloheximide (CHX) (10 μg/ml). (**D**) Block of flagellar regeneration by CrKin13 RNAi. Flagellar regeneration of control and CrKin13 RNAi strains (numbers 92 and 93) was carried out in the presence or absence of CHX (10 μg/ml).

CrKin13, a microtubule depolymerizer, is involved in flagellar assembly (Piao et al., 2009). We reasoned that CrKin13 might depolymerize cytoplasmic microtubules to contribute free tubulins for flagellar assembly. Interestingly, we found that depletion of CrKin13 by RNAi mimicked the effect of taxol. Depletion of CrKin13 by RNAi inhibited flagellar assembly (Fig. 1D) (Piao et al., 2009). In the absence of protein synthesis, however, RNAi strains failed to assemble flagella (Fig. 1C,D). Thus, it indicates that flagellar assembly may involve depolymerization of cytoplasmic microtubules and CrKin13 is an active effector in this process.

Cytoplasmic microtubules depolymerize during flagellar regeneration

To determine that cytoplasmic microtubules are indeed depolymerized during flagellar regeneration, first, we assayed free tubulin changes during flagellar regeneration. Before and after flagellar amputation by pH shock and during flagellar assembly, cell samples were taken at the indicated times and extracted with detergent. The images of cells treated with detergent are shown in supplementary material Fig. S1. Cell

extracts were fractionated into soluble fractions containing free tubulins (S) and insoluble fractions containing microtubules (P) and assayed by SDS-PAGE and immunoblotting with anti-α-tubulin antibody. SksC, a soluble protein, was used as loading control (Kurvari et al., 1996). Immediately after flagellar loss, free tubulins increased as compared to those of pre-deflagellated (pdf) cells (Fig. 2A). During flagellar assembly, free tubulins gradually decreased, and were finally recovered when flagella were assembled to full length, suggesting depletion of cytoplasmic pools of free tubulins for assembly of axonemal microtubules (Fig. 2A).

We further used immunostaining assay to confirm depolymerization of cytoplasmic microtubules at the beginning of flagellar assembly. In control cells, long and dense microtubule fibers emanating from basal bodies were enriched in the cell body (Fig. 2B). In contrast, after flagellar loss, only sparse and shorter microtubules were observed. During the cellular process towards completion of flagellar assembly, cytoplasmic microtubules were gradually recovered (Fig. 4A).

Immediately after deflagellation, new tubulin synthesis starts (Baker et al., 1984; Lefebvre et al., 1980). To determine that the initial increase of free tubulins during flagellar regeneration is not due to new protein synthesis, protein synthesis was blocked by adding 10 μg/ml cycloheximide during flagellar assembly. Microtubule networks and free tubulins were examined by immunostaining and immunoblotting, respectively. In the absence of protein synthesis, increase of free tubulins was observed at 5 min after deflagellation, which was comparable to that of control cells (Fig. 2C). When control cells regenerated full length flagella at 2 h after deflagellation, free tubulins were recovered (Fig. 2C, left panel). As expected, cells treated with cycloheximide did not recover free tubulins (Fig. 2C, right panel). Immunostaining data was consistent with the biochemical assay. Compared with control cells, the cycloheximide treated cells possessed shorter flagella and sparse microtubule arrays even at 2 h after deflagellation (Fig. 2D). These data confirm previous observation that new protein synthesis as well as cytoplasmic pool of flagellar precursors is required for assembly of full length flagella (Rosenbaum et al., 1969).

CrKin13 is required for depolymerization of cytoplasmic microtubules

The inhibition of flagellar assembly by taxol is likely due to stabilization of cytoplasmic microtubules because taxol treated cells did not undergo dramatic depolymerization of cytoplasmic microtubules after flagellar loss (supplementary material Fig. S2). The CrKin13 RNAi data shown in Fig. 1D indicates that CrKin13 is involved in depolymerization of cytoplasmic microtubules. Those RNAi strains were generated by using hairpin DNA sequences to suppress expression of CrKin13 (Piao et al., 2009). Since long hairpin structure might cause non-specific targeting (Schroda, 2006), we have employed artificial microRNA-based strategy to suppress expression of CrKin13 (Molnar et al., 2009). Several strains exhibiting downregulation of expression of CrKin13 were obtained and two of them were analyzed further. Strains mi-32 and mi-25 showed more than 70% decrease of CrKin13 as examined by immunoblot analysis (Fig. 3A) and flagellar assembly of these strains was impaired (Fig. 3B), which is consistent with the results from RNAi strains generated by hairpin DNA sequences though the phenotype was less server (Piao et al., 2009). Next, we analyzed free tubulin

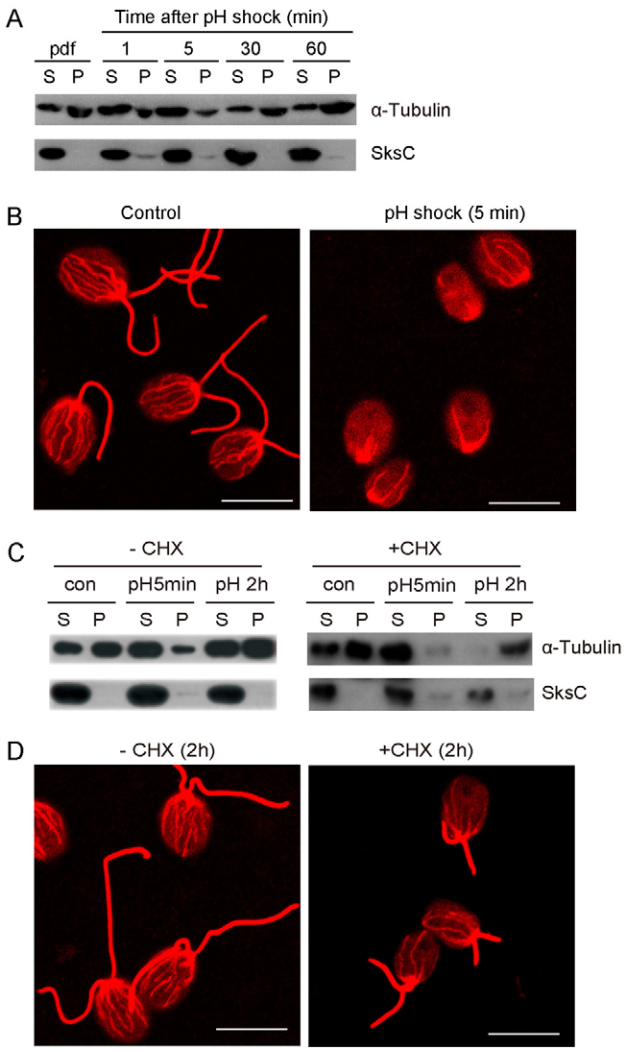

Fig. 2. Depolymerization of cytoplasmic microtubules during flagellar regeneration. (**A**) Immunoblot analysis of free tubulins and polymerized microtubules of cells during flagellar regeneration. Samples taken at the indicated times during flagellar regeneration were fractionated into soluble (S) (containing free tubulins) and insoluble (P) (containing microtubules) fractions followed by immunoblot analysis with antibodies against α-tubulin and SksC. Relative ratios of free tubulins to microtubules were calculated based on densitometry analysis. pdf, pre-deflagellation.
(**B**) Immunofluorescence analysis showing depolymerization of cytoplasmic microtubules after flagellar loss. Control cells and cells at 5 min after deflagellation by pH shock were stained with anti-α-tubulin antibody to visualize microtubules. Scale bars: 10 μm. (**C**) Immunoblot analysis of free tubulins and polymerized microtubules of cells during flagellar regeneration in the presence or absence of CHX. Samples taken at the indicated times were fractionated into soluble (S) and insoluble (P) fractions followed by immunoblot analysis with anti-α-tubulin and anti-SksC antibodies.
(**D**) Immunofluorescence analysis of cytoplasmic microtubules after flagellar regeneration in the presence or absence of CHX. Samples taken at 2 h after pH shock were stained with anti-α-tubulin antibody to visualize cytoplasmic microtubules. Scale bars: 10 μm.

changes during flagellar assembly of these RNAi strains. RNAi strains mi-25 and mi-32 were deflagellated and allowed to regenerate flagella. As shown in Fig. 3C, both RNAi strains did not show increase of free tubulins after flagellar loss. By immunostaining analysis, RNAi cells after flagellar loss

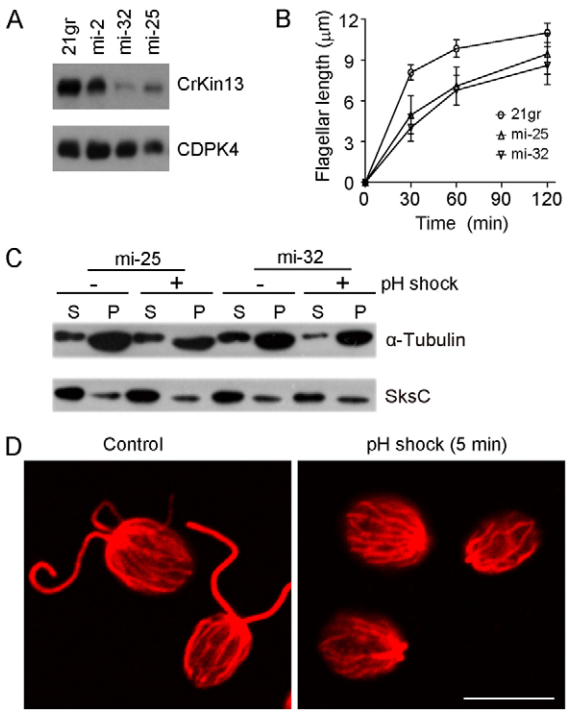

Fig. 3. Cytoplasmic microtubules are not depolymerized in RNAi strains after flagellar loss. (**A**) Knockdown of CrKin13 expression by RNAi. Cell samples were analyzed by immunoblotting with antibodies against anti-CrKin13 and anti-CDPK4, which was used as a loading control. (**B**) Flagellar regeneration in wild type (21gr) and RNAi strains after deflagellation by pH shock. (**C**) Immunoblot analysis of free tubulins and polymerized microtubules of RNAi strains before and after flagellar loss. Cell samples before and after flagellar loss were fractionated and analyzed by immunoblotting as above. (**D**) Immunofluorescence analysis of cytoplasmic microtubules of RNAi strains before (control) and 5 min after flagellar loss induced by pH shock. Samples were stained with anti-α-tubulin. Scale bar: 10 μm.

possessed long and dense microtubule arrays similar to control cells (data from mi-32 is shown) (Fig. 3D). Thus, biochemical and cell biological data support the view that CrKin13 is the effector that mediates depolymerization of cytoplasmic microtubules during flagellar assembly.

Enrichment of CrKin13 in the flagella during rapid phase of flagellar assembly

Our data above show that cytoplasmic microtubule dynamics mediated by CrKin13 provides free tubulins for flagellar assembly. However, flagella themselves are dynamic structures and axonemal microtubules also undergo dynamic changes (Marshall and Rosenbaum, 2001; Song and Dentler, 2001). During rapid phase of flagellar assembly, axonemal microtubule dynamics must be coordinately regulated. In *Tetrahymena*, katanin regulates microtubule dynamics both in the cytoplasm and cilia, and cells lacking katanin assemble short cilia (Sharma et al., 2007). Previously, we have shown that Crkin13 is predominantly localized in the cell body and barely detectable in the flagella of steady state cells (Piao et al., 2009). Thus, we examined possible dynamic association of CrKin13 with the flagella during flagellar assembly. *Chlamydomonas* cells were deflagellated by pH shock and allowed to regenerate flagella. Immunostaining analysis shows that cytoplasmic microtubules were depolymerized during earlier stages of flagellar assembly, and gradually recovered when flagellar assembly was complete (Fig. 4A). CrKin13 was barely detectable in the flagella of steady state cells, as shown previously (Piao et al., 2009). However, during rigorous phase of flagellar assembly at 15 and 30 min after deflagellation, CrKin13 was found to be enriched in the flagella and decreased to normal level in fully assembled flagella (Fig. 4A). Immunoblotting of isolated flagella with anti-CrKin13 and anti-α-tubulin antibodies confirmed this observation (Fig. 4B). The enrichment of CrKin13 in rapidly assembling

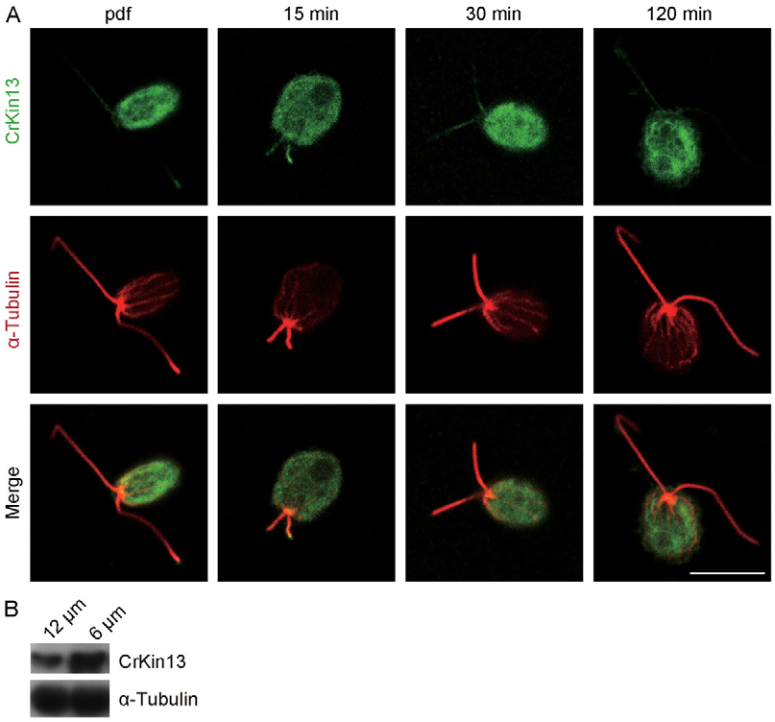

Fig. 4. Enrichment of CrKin13 in the flagella during rapid phase of flagellar assembly. (**A**) Cell samples were taken at the indicated times during flagellar regeneration for immunostaining with antibodies against α-tubulin (red) and CrKin13 (green). Scale bar: 10 μm. (**B**) Flagella from cells regenerating flagella and steady state cells were isolated and subjected to immunoblot analysis with anti-CrKin13 and α-tubulin antibodies, respectively.

flagella may mediate axonemal microtubule dynamics during flagellar assembly.

Phosphorylation of CrKin13 partially inhibits its microtubule depolymerization activity *in vitro*

CrKin13 was phosphorylated during flagellar regeneration (Piao et al., 2009). It has been shown that protein phosphorylation could positively or negatively regulate activity of kinesin-13s (Ems-McClung and Walczak, 2010; Jang et al., 2009). We next asked whether phosphorylation of CrKin13 regulated its activity. By using rhodamine-labeled and taxol-stabilized microtubules and visualization by immunofluorescence, it showed that CrKin13 expressed from insect cells was an active enzyme and depolymerized microtubules in concentration dependent manner (supplementary material Fig. S3A). To determine the effects of phosphorylation on CrKin13 activity, we generated phosphorylated CrKin13 by incubation with *Chlamydomonas* cell lysate because the protein kinase(s) that are responsible for CrKin13 phosphorylation has not been identified (supplementary material Fig. S3B; Fig. 5A). The molecular weight shift indicated phosphorylation of CrKin13, which was confirmed previously (Piao et al., 2009). Rhodamine-labeled taxol-stabilized microtubules were incubated with equal amount of pCrKin13 (phosphorylated CrKin13) and CrKin13, and visualized by immunofluorescence (Lan et al., 2004) (Fig. 5B). The degree of microtubule depolymerization was quantified by counting the number of microtubules per microscope field (Fig. 5C). While buffer alone had no apparent effect, CrKin13 regardless of phosphorylation depolymerized microtubules (Fig. 5B). However, we observed phosphorylated CrKin13 possessed weaker activity as evidenced by less microtubule numbers (Fig. 5C). These data suggest that phosphorylation partially inhibits microtubule depolymerizing activity of CrKin13.

Phosphorylation of CrKin13 regulates its targeting to microtubules

To learn more about the property of CrKin13 regulated by protein phosphorylation, we examined cellular locations of CrKin13. Phosphorylation of MCAK, a member of kinesin-13 family, has been shown to regulate its targeting (Lan et al., 2004). We tested whether phosphorylation of CrKin13 might target it to microtubules. After deflagellation, though most of the cytoplasmic microtubules were depolymerized, sparse and shorter microtubules still existed (Fig. 2B). We set out a cell fractionation assay to test this hypothesis. To do this, control cells and deflagellated cells were lysed and fractionated into soluble fractions (S) and insoluble microtubule containing fractions (P). The samples were then analyzed by SDS-PAGE and immunoblotting. Control protein SksC was localized to the soluble fractions from control and deflagellated cells (Fig. 6A). CrKin13 was not phosphorylated in control cells and localized to the soluble fraction. In contrast, Crkin13 was phosphorylated in deflagellated cells and was solely present in the insoluble fraction (Fig. 6A). Analysis of cell samples taken at different stages of flagellar assembly when CrKin13 underwent phosphorylation changes also showed that pCrKin13 was localized to the insoluble fraction while CrKin13 to the soluble fraction (Fig. 6B).

We have used phosphorylation and dephosphorylation assay to further show that phosphorylation was a key factor in targeting CrKin13 to cytoplasmic microtubules. Control cells were lysed in the presence of ATP to induce CrKin13 phosphorylation. Cell fractionation and immunoblotting showed that CrKin13 was

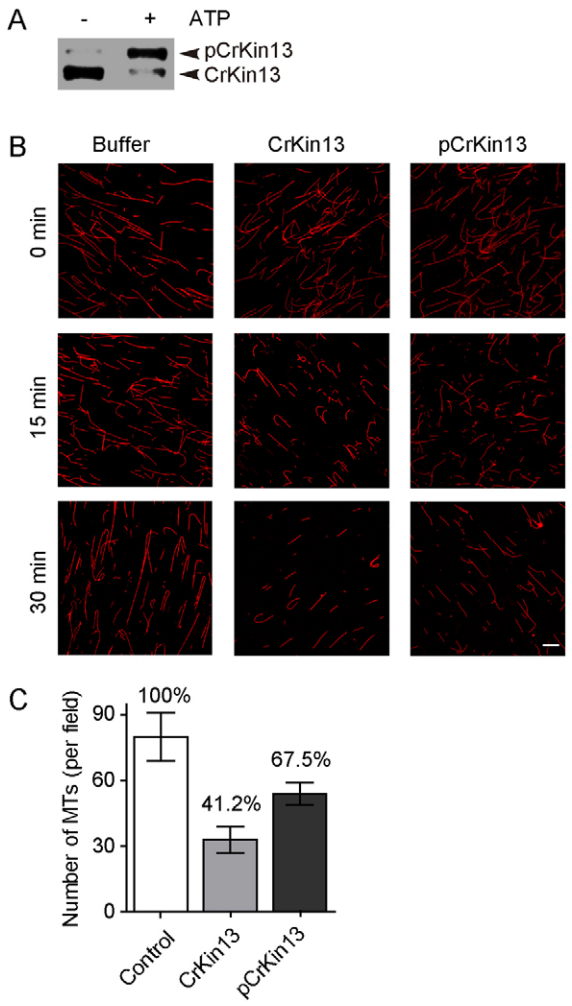

Fig. 5. Phosphorylation inhibits CrKin13 activity *in vitro*. (**A**) Immunoblotting showing that CrKin13 expressed in insect cells was induced to be phosphorylated by incubation with deflagellated cell lysate in the presence of ATP. (**B**) Visualization of microtubule depolymerization by CrKin13. Rhodamine-labeled, taxol-stabilized microtubules were incubated with 1 μM phosphorylated or non-phosphorylated CrKin13 for the indicated times. Scale bar: 10 μm. (**C**) Quantification of *in vitro* CrKin13 activity. The graph shows the number of microtubules per field for the 30 min time point in B. Error bars: ±s.d.

localized to the microtubule fractions when it became phosphorylated (Fig. 6C). Reversely, when pCrKin13 from the deflagellated cell lysate became dephosphorylated by phosphatase treatment, it changed its location from free soluble fraction to insoluble fraction (Fig. 6D).

To further confirm that the localization of pCrKin13 to the insoluble fraction was due to association with microtubules, cells were lysed under cold condition, which supposedly depolymerizes most cytoplasmic microtubules except acetylated rootlet microtubules (Holmes and Dutcher, 1989; LeDizet and Piperno, 1986). Indeed, pCrKin13 was localized in the soluble fraction after microtubule depolymerization (Fig. 6E).

Phosphorylation at S100 of CrKin13 regulates its targeting to microtubules

To learn the phosphorylation mechanisms of CrKin13, we determined the phosphorylated residues in pCrKin13 by mass

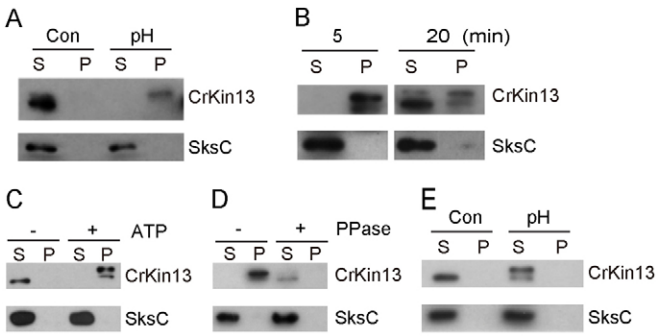

Fig. 6. Phosphorylation of CrKin13 regulates its targeting to cytoplasmic microtubules *in vivo*. (**A**) Control (con) and deflagellated cells induced by pH shock (pH) were fractionated into soluble (S) and insoluble (P) fractions followed by immunoblot analysis with antibodies against CrKin13 and SksC. (**B**) Cells during flagellar regeneration at the indicated time from flagellar loss induced by pH shock were fractionated into soluble (S) and insoluble (P) fractions followed by immunoblot analysis. (**C**) Control cells were lysed in buffer and incubated for 30 min at room temperature in the presence or absence of 1 mM ATP. Cell lysates were then fractionated into soluble (S) and insoluble (P) fractions followed by immunoblot analysis. (**D**) Cell lysates from deflagellated cells induced by pH shock were treated with or without alkaline phosphatase and then fractionated into soluble (S) and insoluble (P) fractions, which were subjected to immunoblot analysis. (**E**) Control and deflagellated cells were first treated with cold to allow microtubule depolymerization and then fractionated into soluble (S) and insoluble (P) fractions followed by immunoblot analysis.

spectrometry. Anti-MPM2 antibody has been shown to recognize and be able to immunoprecipitate pCrKin13 (Piao et al., 2009). pCrKin13 was immunoprecipitated using anti-MPM2 antibody conjugated beads from deflagellated cells. Immunoprecipitation from control cells was used as control. The immunoprecipitates from anti-MPM2 beads were analyzed on SDS-PAGE and Coomassie Blue staining (Fig. 7A). The pCrKin13 band (arrow) was excised and digested by trypsin followed by mass spectrometry analysis. Residues S100 and S522 were identified to be phosphorylated while T469 was potentially phosphorylated (supplementary material Fig. S4 and data not shown). S100 was localized in the N-terminal domain while S522 in the C-terminal domain (Fig. 7B).

We focused on whether phosphorylation would affect CrKin13 targeting to microtubules because phosphorylation was absolutely required. First, we examined the role of S522 and T469 phosphorylations by making point mutations. HA-tagged CrKin13 constructs with double mutation or not were expressed in *Chlamydomonas* wild type cells, respectively. After deflagellation induced by pH shock, double mutants CrKin13–HA-T469A-S522A still underwent gel-shift as control CrKin13–HA in an immunoblot assay (Fig. 7C). Analysis by cell fractionation followed by immunoblotting showed that these mutations did not affect its association with microtubules either (Fig. 7D). SksC was used as control. Thus, S522 and T469 phosphorylation was not responsible for gel-shift associated phosphorylation of CrKin13 and not required for CrKin13 targeting as well.

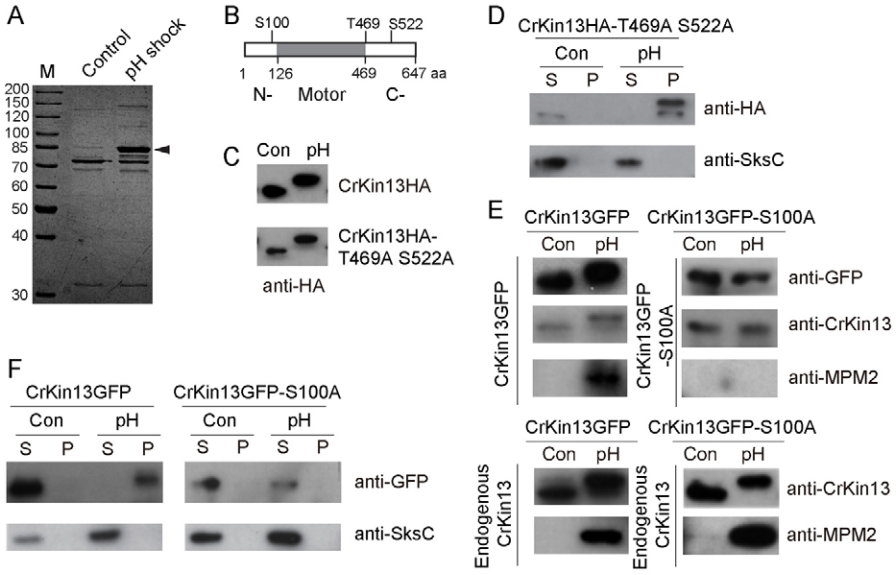

Fig. 7. Phosphorylation at S100 of CrKin13 is required for its targeting to cytoplasmic microtubules. (**A**) Immunoprecipitation of phosphorylated CrKin13 for mass spectrometry. Immunoprecipitates obtained by using anti-MPM2 antibody from control and deflagellated cells were analyzed by SDS PAGE and Coomassie Blue staining. The indicated band (arrowhead) was excised for identification of phosphorylation sites by mass spectrometry. (**B**) Diagram showing domains and phosphorylation residues of CrKin13 determined by mass spectrometry. N-, N-terminal domain; motor, motor domain; C-, C-terminal domain. (**C**) Strains expressing CrKin13–HA and CrKin13–HA-T469A-S522A were deflagellated by pH shock (pH) or not (Con) followed by immunoblotting with anti-HA antibody. (**D**) Control (Con) and pH-shock-treated cells expressing CrKin13–HA-T469A-S522A were fractionated into soluble (S) and insoluble (P) fractions followed by immunoblot analysis with anti-HA and anti-SksC antibodies, respectively. (**E**) Immunoblot analysis of control (Con) and pH-shock-treated cells (pH) expressing CrKin13–GFP or CrKin13–GFP-S100A. Upper panels: analysis of GFP-tagged CrKin13s with anti-GFP, anti-CrKin13, and anti-MPM2 antibodies. Lower panels: analysis of endogenous CrKin13 with anti-CrKin13 and anti-MPM2 antibodies. (**F**) Control (Con) and pH-shock-treated cells (pH) expressing CrKin13–GFP or CrKin13–GFP-S100A were fractionated into soluble (S) and insoluble (P) fractions followed by immunoblot analysis with anti-GFP and anti-SksC antibodies, respectively.

Next, we examined whether S100 phosphorylation was responsible for gel-shift associated phosphorylation of CrKin13 and required for targeting to microtubules. GFP-tagged CrKin13 or CrKin13-S100A was expressed in *Chlamydomonas*. In strains expressing CrKin13–GFP, after deflagellation by pH shock, endogenous CrKin13 as well as CrKin13–GFP exhibited phosphorylation rendered gel-shift as demonstrated by anti-GFP and anti-CrKin13 antibodies in immunoblot analysis (Fig. 7E). Anti-MPM2 antibody identified the gel-shifted CrKin13 and CrKin13–GFP as being phosphorylated. In strains expressing CrKin13–GFP-S100A, endogenous CrKin13 as expected showed gel-shift and was phosphorylated after flagellar loss as detected by anti-CrKin13 and anti-MPM2 antibodies. In contrast, CrKin13–GFP-S100A did not undergo gel-shift and was not recognized by anti-MPM2 antibody (Fig. 7E). These data suggest that S100 is phosphorylated during deflagellation, and is also the phosphorylated site recognized by anti-MPM2 antibody.

To determine whether S100 phosphorylation is required for microtubule targeting of CrKin13, Strains expressing CrKin13–GFP and CrKin13–GFP-S100A were lysed, fractionated and the location of tagged forms of CrKin13 was analyzed by SDS-PAGE and immunoblotting. CrKin13–GFP became phosphorylated after deflagellation, and localized to the insoluble fraction, whereas CrKin13–GFP of control cells was not phosphorylated and localized to the soluble fraction (Fig. 7F). In contrast, CrKin13–GFP-S100A was not phosphorylated after deflagellation. As expected, it was localized to the soluble fraction (Fig. 7F). Thus, phosphorylation at S100 is essential for gel-shift associated phosphorylation of CrKin13 and required for microtubule targeting of CrKin13 during flagellar assembly.

Discussion

Cilia and flagella are microtubule based structures. The assembly of cilia and flagella require not only protein synthesis but also free flagellar precursors including tubulins in the cytoplasm. In this study, we demonstrated that CrKin13, a microtubule depolymerizer, depolymerizes cytoplasmic microtubules to provide free tubulins for flagellar assembly and protein phosphorylation of CrKin13 at residue S100 controls its targeting to microtubules.

Cytoplasmic microtubules serve as a 'cytoplasmic pool' for tubulin precursors during flagellar regeneration

After amputation of cilia and flagella, cells quickly reassemble them, which have been demonstrated in several model systems including sea urchin embryo (Auclair and Siegel, 1966), *Tetrahymena* (Rosenbaum and Carlson, 1969), *Chlamydomonas* (Rosenbaum et al., 1969) and several protozoan flagellates (Rosenbaum and Child, 1967). Subsequent studies showed that the cells possess large quantities of flagellar precursors that can be used for flagellar assembly (reviewed by Lefebvre and Rosenbaum, 1986). Tubulin is the major component of cilia and flagella. In sea urchin embryo, large quantities of tubulin along with other flagellar precursors are present that are sufficient for cilia assembly in the absence of protein synthesis (Raff et al., 1971; Stephens, 1977). Studies in *Tetrahymena* show that synthesis of tubulin only starts when cells regain cilia-based motility (Guttman and Gorovsky, 1979). In *Chlamydomonas*, cells reassemble half-length of flagella after flagellar amputation in the absence of protein synthesis, indicating tubulins for assembly of axonemal microtubules come from cytoplasmic pool (Rosenbaum et al., 1969). We show that prior to flagellar regeneration cytoplasmic microtubules were depolymerized as evidenced by biochemical and cytological data, and taxol, which stabilizes microtubules, impaired flagellar regeneration and flagellar elongation. Furthermore, in the absence of protein synthesis Taxol almost blocked flagellar regeneration. These data suggest that depolymerization of cytoplasmic microtubules provide tubulin precursors for flagellar assembly. This finding is consistent with results from mammalian cells. Taxol treatment reduces cilia length of ciliated cells, and inhibits assembly of new cilia, whereas nocodazole treatment increases cilia length. Furthermore, changes of actin dynamics by pharmacological drugs induce cilia elongation with concomitant increase of free tubulins (Sharma et al., 2011).

Free tubulins in the cytoplasm are delivered to the flagellar tip for assembly (Johnson and Rosenbaum, 1992; Marshall and Rosenbaum, 2001). In *C. elegans*, axoneme-specific tubulin isotypes are transported to cilia for assembly (Hao et al., 2011). In *Chlamydomonas*, two pairs of α- and β-tubulin genes exist, and each pair produces almost identical proteins, indicating that the same tubulin dimmer is used for both cytoplasmic and axonemal microtubules (Silflow et al., 1985; Youngblom et al., 1984). Flagellar length control has been explained by the balance point model, where IFT mediated flagellar assembly by delivering flagellar precursors to the flagellar tip balances with disassembly (Marshall and Rosenbaum, 2001). The cytoplasmic pool of tubulins may not be the limiting factor for flagellar length because steady state cells possess extra tubulins that are sufficient for assembly half-length of flagella (Rosenbaum and Carlson, 1969). Interestingly, tektin, a non-tubulin flagellar protein, has been found to be synthesized *de novo* during cilia regeneration in sea urchin, and proposed to be a limiting component of the cytoplasmic pool for cilia regeneration and cilia length (Norrander et al., 1995).

CrKin13 acts as an effector to regulate cytoplasmic microtubule depolymerization during flagellar regeneration

In vitro assay shows that CrKin13 is an active microtubule depolymerizer. CrKin13 RNAi strains were defective in depolymerization of cytoplasmic microtubules. And in the absence of protein synthesis, depletion of CrKin13 by RNAi blocked flagellar assembly, suggesting that depolymerization of cytoplasmic microtubule mediated by CrKin13 provides tubulins for assembly of axonemal microtubules. Recent studies show that kinesin-13s play a role in flagellar length control. In *Leishmania*, overexpression of LmjKIN3-2 results in shorter flagella, whereas its knockdown produces longer flagella (Blaineau et al., 2007). Ectopic expression of an inactive kinesin-13 mutant in *Giardia* causes longer flagella (Dawson et al., 2007). These data, collectively with our finding, indicate that kinesin-13 plays a conserved role in flagellar assembly and length control. However, the fact that knockdown of CrKin13 induces shorter flagella in *Chlamydomonas* suggests that the regulation of microtubule dynamics by kinesin-13s in flagellar control is diversified. The distinct functions of CrKin13 and LmjKIN3-2 may be attributed to specific localization of these molecules. LmjKIN3-2 is exclusively localized to the flagella in *Leishmania* (Blaineau et al., 2007) whereas CrKin13 is predominantly localized to the cell body (Piao et al., 2009). In *Giardia*, treatments with taxol and nocodazole induce flagellar length changes (Dawson et al., 2007), however, no effects were found in *Chlamydomonas*.

Regulation of CrKin13 by protein phosphorylation

We showed that CrKin13 was phosphorylated during depolymerization of cytoplasmic microtubules. And phosphorylation of CrKin13 partially inhibited its activity and was absolutely required for its targeting to microtubules. The regulation of activity and location by protein phosphorylation has been shown in other members of kinesin-13 family (Ems-McClung and Walczak, 2010). The centromeric MCAK is required for microtubule dynamics to control chromosome congression and segregation (Maney et al., 2001; Walczak et al., 2002). Protein phosphorylation of MCAK by aurora B inhibits its activity and targets it to centromere (Lan et al., 2004). It has been proposed that phosphorylation induces its targeting to centromere and dephosphorylation whereon activates its activity to control microtubule dynamics. CrKin13 may be regulated in similar manner. We propose that the location control of CrKin13 prevents active CrKin13 from depolymerizing cytoplasmic microtubules in steady state cells. During flagellar regeneration, CrKin13 becomes phosphorylated and targeted to microtubules to exert its activity through unknown dephosphorylation process, thus providing delicate control of microtubule dynamics. Protein kinases that phosphorylate kinesin-13s include aurora A, aurora B and Plk1 (Hood et al., 2012; Jang et al., 2009; Lan et al., 2004). The kinase that phosphorylates CrKin13 is unknown. One candidate is the aurora-like kinase CALK which undergoes protein phosphorylation during flagellar assembly (Pan et al., 2004). We are currently exploring this possibility.

Materials and Methods

Strains and special chemicals

Chlamydomonas reinhardtii strains *21gr* (mt+) (CC-1690) is available from the *Chlamydomonas* Genetics Center, University of Minnesota. Cycloheximide (CHX), taxol, nocodazole and ATP-Mg (Sigma, St. Louis, MO) were used at concentrations indicated in the text.

Cell culture, deflagellation, flagellar regeneration, flagellar isolation and flagellar length measurements

Growing of vegetative cells is described elsewhere (Piao et al., 2009). Briefly, vegetative cells grown in liquid M medium were cultured at 23℃ with aeration under 14:10 h light–dark cycle. Deflagellation by pH shock, flagellar isolation, flagellar regeneration and flagellar length measurement are essentially as described previously (Luo et al., 2011). Briefly, cells were deflagellated by pH shock and allowed for flagellar regeneration. Control cells and cells during flagellar regeneration were fixed with 1% glutaraldehyde and imaged by differential interference contrast microscopy with a 40× objective lens on a Zeiss Axio Observer Z1 microscope (Carl Zeiss, Germany) equipped with a camera (QuantEM 512SC, Photometrics, USA). Flagellar length was measured by using ImageJ (NIH, USA) and calibrated with a micrometer. For each time point, flagella from at least 50 cells were measured. Flagellar length was graphed using GraphPad Prism 5.01 (GraphPad, USA).

Nucleic acid manipulations, RNAi design and *Chlamydomonas* transformations

General molecular protocols were used for nucleic acid manipulations and all the constructs were confirmed by sequencing. To express HA-tagged CrKin13 and CrKin13-T469A-S522A, and GFP-tagged CrKin13 and CrKin13-S100A in *Chlamydomonas*, genomic DNA sequences with endogenous promoter were used to make the constructs. HA and GFP tags were at the C terminus of CrKin13. For antibiotic selection of *Chlamydomonas* transformants, an expression cassette of the paromomycin-resistance gene *aphVIII* from plasmid pIS103 (Sizova et al., 2001) was cloned into the above constructs. An electroporation method was used to transform the above constructs and microRNA constructs (below) into *Chlamydomonas* (Shimogawara et al., 1998). Positive transformants were selected by immunoblotting with anti-HA antibody or anti-GFP antibody, respectively.

The RNAi strains generated by using hairpin DNA sequences were obtained from previous work (Piao et al., 2009). To design microRNA constructs to suppress CrKin13 expression, the procedures from WMD3 [Web MicroRNA Designer (Web MicroRNA Designer (http://wmd3.weigelworld.org)] were followed. The target sequence (TTTAGCCTTGAATGTGTCCAT) at 3′ coding sequence of CrKin13 was selected for insertion into the *Spe*I site of the artificial MicroRNA vector pChlamiRNA3int. The 90 bp oligonucleotides were as follows: amiFor_CrKin13-2 ctagtATGGACACATTCAAGGGTAAAtctcgctgatcggcaccatg-ggggtggtggtgatcagcgctaTTTAGCCTTGAATGTGTCCATg; and amiRev_CrKin13-2 ctagcATGGACACATTCAAGGCTAAAtagcgctgatcaccaccacccccatggtgccgatcagc-gagaTTTACCCTTGAATGTGTCCATa. The microRNA construct pChlamiRNA3 int-CrKin13-2 was linearized with *Dra*I and was transformed by electroporation into *Chlamydomonas*. The transformants were screened by immunoblotting with anti-CrKin13 antibody.

Expression of CrKin13 in insect cells

Baculovirus expression system was used for expression of CrKin13 in Sf-9 insect cells. CrKin13 cDNA was amplified by PCR with flanking *Bam*HI and *Sal*I sites. The fragment was cloned into modified pFastBac^{TM}1 (Invitrogen, USA) vector with 6×His tag. His-tagged CrKin13 was purified on a HisTrap HP column followed by ion-exchange column HiTrap SP and gel filtration column Superdex200 10/300 GL (GE, USA). The protein was eluted in 1× BRB80 buffer (80 mM PIPES, 1 mM $MgCl_2$, 1 mM EGTA, pH 6.8 adjusted with KOH) containing 1 mM DTT, 10 μM ATP-Mg. Sucrose was added to 10% and the samples were flash frozen in liquid nitrogen and stored at 80℃ until use. The protein concentration was determined with Protein Assay Dye Reagent Concentrate (Bio-Rad, USA).

Assay of microtubule depolymerization activity

Microtubule polymerization was performed according to previously published method (Li et al., 2011). Briefly, tubulin proteins purified from porcine brain were clarified by ultra-centrifugation in TLA100 rotor of table-top ultracentrifuge (Beckman, USA) at 100,000×g for 10 min at 2℃. For polymerization of microtubules, NHS-rhodamine-labeled tubulins were first incubated at 37℃ for 1–2 min, followed by stepwise addition of taxol. The protein concentration of the taxol-stabilized microtubules was determined by Protein Assay Dye Reagent Concentrate (Bio-Rad, USA) and a final concentration of 20 μM was adjusted with BRB80 containing 1 mM DTT and 20 μM taxol.

To prepare phosphorylated CrKin13, purified CrKin13 was incubated with deflagellated cell lysate in the presence of 1 mM ATP. Deflagellated cells were lysed in HMDEK buffer (20 mM HEPES, pH 7.2, 5 mM $MgCl_2$, 1 mM DTT, 1 mM EDTA, 25 μg/ml ALLN [Roche, USA], EDTA-free protease inhibitor cocktail [Roche]). Different amounts (0–8 μg) of clear cell lysates resulted from centrifugation at 14,000 rpm for 5 min at 4℃ were mixed with 8 μg CrKin13 in a final volume of 10 μl in the presence of 1 mM ATP, and incubated at 30℃ for 30 min.

For the fluorescence microtubule assays, CrKin13 or pCrKin13 was incubated with polymerized microtubules in BRB80 buffer containing 1 mM ATP at room temperature. The samples above were viewed and acquired by Zeiss 510 META Confocal Laser Microscope and images were analyzed with Photoshop (Adobe, USA).

Cell fractionation for free tubulins and microtubules

For determination of free tubulins and intact microtubule from cells, a modification of previously published method was used (Loktev et al., 2008). 1 ml of cells with 5×10^6 cells/ml was collected by centrifugation at 6000 rpm for 1 min at room temperature. The cell pellet was resuspended in 25 μl TMMET buffer (20 mM Tris-HCl, pH 6.8, 0.14 M NaCl, 1 mM $MgCl_2$, 2 mM EGTA, 4 μg/ml Taxol, 0.5% NP40) with pipetting for 2–5 min, followed by centrifugation at 14,000 rpm for 10 min at room temperature. Equal proportions of the supernatant and the pellet were boiled in 1× SDS sample buffer followed by SDS-PAGE and immunoblot analysis.

Immunoprecipitation

To immunoprecipitate CrKin13 for mass-spectrometry analysis, 2×10^8 deflagellated or control cells were lysed with buffer A (20 mM HEPES, pH 7.2, 5 mM $MgCl_2$, 1 mM DTT, 1 mM EDTA, 20 mM β-glycerol phosphate, 10 mM NaF, 0.1 mM Na_3VO_4, 150 mM NaCl, 5% glycerol, EDTA-free protease inhibitor cocktail and 25 μg/ml ALLN). The clear cell lysates after centrifugation were first cleared by protein A beads followed by addition of 50 μl mouse anti-MPM2 conjugated beads (Upstate, USA) and incubation in ice with shaking for 2 h. After washing four times with buffer A containing 0.1% NP40 and 0.1% Triton X-100 and one time with Tris buffer (10 mM Tris, pH 7.5), the beads were boiled in 1× SDS sample buffer for 5 min, and analyzed by SDS-PAGE followed by Coomassie Blue staining. The protein band was subject to mass spectrometry analysis.

SDS-PAGE and immunoblotting

SDS-PAGE and immunoblotting were essentially as described previously (Piao et al., 2009). Cell or protein samples were dissolved in buffer A, and boiled in 1× SDS sample buffer for 5 min and analyzed by SDS-PAGE and immunoblotting. For phosphatase treatment of phosphorylated CrKin13, alkaline phosphatase (New England Biolabs, USA) was used (Piao et al., 2009). The antibodies used for

immunoblotting are as follows: rabbit anti-CrKin13 (1:3000) (Piao et al., 2009), anti-SksC (1:2000) (kindly provided by Dr William Snell), anti-CDPK4 (1:5000), mouse anti-MPM2 (1:3000) (Millipore, USA), anti-GFP (1:3000) (Abmart, China), anti-α-tubulin (1:5000) (Sigma, USA), and rat anti-HA (1:1000) (Roche, Switzerland). Densitometry of immunoblot was analyzed with TotalLab-Software (Nonlinear Dynamics Ltd, UK).

Immuofluorescence microscopy

Cells in M medium were collected by centrifugation, resuspended in MT buffer (30 mM HEPES [pH 7.2], 3 mM EGTA, 1 mM MgSO4, 25 mM KCl), fixed for 5 min at room temperature in MT buffer containing 4% paraformaldehyde. The fixed cells were resuspended in MT buffer with 0.5% NP40 for 2 min at room temperature. The samples were further extracted in 100% methanol for 5–10 min at −20℃. The samples were then processed following previously published method (Piao et al., 2009). Primary antibodies were anti-α-tubulin (1:100) and anti-CrKin13 (1:50) and secondary antibodies Texas Red goat anti-mouse IgG (1:400) and Alexa Fluor 488 goat anti-rabbit IgG (1:400) (Molecular Probes). Samples were imaged on a Zeiss710 META Observer Z1 Confocal Laser Microscope (Zeiss, Germany). Images were acquired and processed by ZEN 2009 Light Edition software and Photoshop, and assembled in Adobe Illustrator (Adobe, USA).

Analysis of phosphorylation sites by mass spectrometry

The immunoprecipitated pCrKin13 was analyzed on SDS-PAGE and stained with Coomassie Blue. The gel band was excised from the gel, reduced with 10 mM DTT and alkylated with 55 mM iodoacetamide, and digested with trypsin (Promega, Fitchburg, WI) in 50 mM ammonium bicarbonate at 37℃ overnight. The peptides were extracted twice with 1% trifluoroacetic acid in 50% acetonitrile aqueous solution for 30 min. The extractions were then centrifuged in a speedvac to reduce the volume. For LC-MS/MS analysis, the digestion product was separated by a 65 min gradient elution at a flow rate 0.25 µl/min with the EASY-nLCII^{TM} integrated nano-HPLC system (Proxeon, Denmark), which is directly interfaced with the Thermo LTQ-Orbit trap mass spectrometer (Thermo, USA). The MS/MS spectra from each LC-MS/MS run were searched against the selected database using an in-house Mascot or Proteome Discovery searching algorithm.

Acknowledgements

We thank Dr Ming Yuan for providing materials and helpful discussions.

Author contributions

L.W., T.P., M.C., T.Q., L.H., H.D., T.M. and J.P. designed the experiments and analyzed the data. L.W., T.P., M.C., T.Q. and H.D. conducted the experiments. L.W. and J.P. wrote the paper.

Funding

This work was supported by the National Basic Research Program of China (973 program) [grant numbers 2012CB945003, 2013CB910700]; and the National Natural Science Foundation of China [grant numbers 30830057, 30988004] (all to J.P.).

Supplementary material available online at
http://jcs.biologists.org/lookup/suppl/doi:10.1242/jcs.124255/-/DC1

References

Auclair, W. and Siegel, B. W. (1966). Cilia regeneration in the sea urchin embryo: evidence for a pool of ciliary proteins. *Science* **154**, 913-915.

Baker, E. J., Schloss, J. A. and Rosenbaum, J. L. (1984). Rapid changes in tubulin RNA synthesis and stability induced by deflagellation in Chlamydomonas. *J. Cell Biol.* **99**, 2074-2081.

Blaineau, C., Tessier, M., Dubessay, P., Tasse, L., Crobu, L., Pagès, M. and Bastien, P. (2007). A novel microtubule-depolymerizing kinesin involved in length control of a eukaryotic flagellum. *Curr. Biol.* **17**, 778-782.

Brown, D. L. and Bouck, G. B. (1973). Microtubule biogenesis and cell shape in Ochromonas. II. The role of nucleating sites in shape development. *J. Cell Biol.* **56**, 360-378.

Carvalho-Santos, Z., Azimzadeh, J., Pereira-Leal, J. B. and Bettencourt-Dias, M. (2011). Evolution: Tracing the origins of centrioles, cilia, and flagella. *J. Cell Biol.* **194**, 165-175.

Christensen, S. T., Pedersen, L. B., Schneider, L. and Satir, P. (2007). Sensory cilia and integration of signal transduction in human health and disease. *Traffic* **8**, 97-109.

Dawson, S. C., Sagolla, M. S., Mancuso, J. J., Woessner, D. J., House, S. A., Fritz-Laylin, L. and Cande, W. Z. (2007). Kinesin-13 regulates flagellar, interphase, and mitotic microtubule dynamics in Giardia intestinalis. *Eukaryot. Cell* **6**, 2354-2364.

Ems-McClung, S. C. and Walczak, C. E. (2010). Kinesin-13s in mitosis: Key players in the spatial and temporal organization of spindle microtubules. *Semin. Cell Dev. Biol.* **21**, 276-282.

Goetz, S. C. and Anderson, K. V. (2010). The primary cilium: a signalling centre during vertebrate development. *Nat. Rev. Genet.* **11**, 331-344.

Guttman, S. D. and Gorovsky, M. A. (1979). Cilia regeneration in starved tetrahymena: an inducible system for studying gene expression and organelle biogenesis. *Cell* **17**, 307-317.

Hao, L., Thein, M., Brust-Mascher, I., Civelekoglu-Scholey, G., Lu, Y., Acar, S., Prevo, B., Shaham, S. and Scholey, J. M. (2011). Intraflagellar transport delivers tubulin isotypes to sensory cilium middle and distal segments. *Nat. Cell Biol.* **13**, 790-798.

Holmes, J. A. and Dutcher, S. K. (1989). Cellular asymmetry in Chlamydomonas reinhardtii. *J. Cell Sci.* **94**, 273-285.

Hood, E. A., Kettenbach, A. N., Gerber, S. A. and Compton, D. A. (2012). Plk1 regulates the kinesin-13 protein Kif2b to promote faithful chromosome segregation. *Mol. Biol. Cell* **23**, 2264-2274.

Ishikawa, H. and Marshall, W. F. (2011). Ciliogenesis: building the cell's antenna. *Nat. Rev. Mol. Cell Biol.* **12**, 222-234.

Jang, C. Y., Coppinger, J. A., Seki, A., Yates, J. R., 3rd and Fang, G. (2009). Plk1 and Aurora A regulate the depolymerase activity and the cellular localization of Kif2a. *J. Cell Sci.* **122**, 1334-1341.

Johnson, K. A. and Rosenbaum, J. L. (1992). Polarity of flagellar assembly in Chlamydomonas. *J. Cell Biol.* **119**, 1605-1611.

Kim, J., Lee, J. E., Heynen-Genel, S., Suyama, E., Ono, K., Lee, K., Ideker, T., Aza-Blanc, P. and Gleeson, J. G. (2010). Functional genomic screen for modulators of ciliogenesis and cilium length. *Nature* **464**, 1048-1051.

Kurvari, V., Zhang, Y., Luo, Y. and Snell, W. J. (1996). Molecular cloning of a protein kinase whose phosphorylation is regulated by genetic adhesion during Chlamydomonas fertilization. *Proc. Natl. Acad. Sci. USA* **93**, 39-43.

Lan, W., Zhang, X., Kline-Smith, S. L., Rosasco, S. E., Barrett-Wilt, G. A., Shabanowitz, J., Hunt, D. F., Walczak, C. E. and Stukenberg, P. T. (2004). Aurora B phosphorylates centromeric MCAK and regulates its localization and microtubule depolymerization activity. *Curr. Biol.* **14**, 273-286.

LeDizet, M. and Piperno, G. (1986). Cytoplasmic microtubules containing acetylated alpha-tubulin in Chlamydomonas reinhardtii: spatial arrangement and properties. *J. Cell Biol.* **103**, 13-22.

Lefebvre, P. A. and Rosenbaum, J. L. (1986). Regulation of the synthesis and assembly of ciliary and flagellar proteins during regeneration. *Annu. Rev. Cell Biol.* **2**, 517-546.

Lefebvre, P. A., Silflow, C. D., Wieben, E. D. and Rosenbaum, J. L. (1980). Increased levels of mRNAs for tubulin and other flagellar proteins after amputation or shortening of Chlamydomonas flagella. *Cell* **20**, 469-477.

Li, J., Wang, X., Qin, T., Zhang, Y., Liu, X., Sun, J., Zhou, Y., Zhu, L., Zhang, Z., Yuan, M. et al. (2011). MDP25, a novel calcium regulatory protein, mediates hypocotyl cell elongation by destabilizing cortical microtubules in Arabidopsis. *Plant Cell* **23**, 4411-4427.

Loktev, A. V., Zhang, Q., Beck, J. S., Searby, C. C., Scheetz, T. E., Bazan, J. F., Slusarski, D. C., Sheffield, V. C., Jackson, P. K. and Nachury, M. V. (2008). A BBSome subunit links ciliogenesis, microtubule stability, and acetylation. *Dev. Cell* **15**, 854-865.

Luo, M., Cao, M., Kan, Y., Li, G., Snell, W. and Pan, J. (2011). The phosphorylation state of an aurora-like kinase marks the length of growing flagella in Chlamydomonas. *Curr. Biol.* **21**, 586-591.

Maney, T., Wagenbach, M. and Wordeman, L. (2001). Molecular dissection of the microtubule depolymerizing activity of mitotic centromere-associated kinesin. *J. Biol. Chem.* **276**, 34753-34758.

Marshall, W. F. and Rosenbaum, J. L. (2001). Intraflagellar transport balances continuous turnover of outer doublet microtubules: implications for flagellar length control. *J. Cell Biol.* **155**, 405-414.

McNally, F. J. and Vale, R. D. (1993). Identification of katanin, an ATPase that severs and disassembles stable microtubules. *Cell* **75**, 419-429.

Mennella, V., Rogers, G. C., Rogers, S. L., Buster, D. W., Vale, R. D. and Sharp, D. J. (2005). Functionally distinct kinesin-13 family members cooperate to regulate microtubule dynamics during interphase. *Nat. Cell Biol.* **7**, 235-245.

Molnar, A., Bassett, A., Thuenemann, E., Schwach, F., Karkare, S., Ossowski, S., Weigel, D. and Baulcombe, D. (2009). Highly specific gene silencing by artificial microRNAs in the unicellular alga Chlamydomonas reinhardtii. *Plant J.* **58**, 165-174.

Nakamura, S., Takino, H. and Kojima, M. K. (1987). Effect of lithium on flagellar length in Chlamydomonas reinhardtii. *Cell Struct. Funct.* **12**, 369-374.

Norrander, J. M., Linck, R. W. and Stephens, R. E. (1995). Transcriptional control of tektin A mRNA correlates with cilia development and length determination during sea urchin embryogenesis. *Development* **121**, 1615-1623.

Ou, Y., Ruan, Y., Cheng, M., Moser, J. J., Rattner, J. B. and van der Hoorn, F. A. (2009). Adenylate cyclase regulates elongation of mammalian primary cilia. *Exp. Cell Res.* **315**, 2802-2817.

Pan, J., Wang, Q. and Snell, W. J. (2004). An aurora kinase is essential for flagellar disassembly in Chlamydomonas. *Dev. Cell* **6**, 445-451.

Pazour, G. J. and Witman, G. B. (2003). The vertebrate primary cilium is a sensory organelle. *Curr. Opin. Cell Biol.* **15**, 105-110.

Piao, T., Luo, M., Wang, L., Guo, Y., Li, D., Li, P., Snell, W. J. and Pan, J. (2009). A microtubule depolymerizing kinesin functions during both flagellar disassembly and flagellar assembly in Chlamydomonas. *Proc. Natl. Acad. Sci. USA* **106**, 4713-4718.

Qin, H., Diener, D. R., Geimer, S., Cole, D. G. and Rosenbaum, J. L. (2004). Intraflagellar transport (IFT) cargo: IFT transports flagellar precursors to the tip and turnover products to the cell body. *J. Cell Biol.* **164**, 255-266.

Raff, R. A., Greenhouse, G., Gross, K. W. and Gross, P. R. (1971). Synthesis and storage of microtubule proteins by sea urchin embryos. *J. Cell Biol.* **50**, 516-527.

Remillard, S. P. and Witman, G. B. (1982). Synthesis, transport, and utilization of specific flagellar proteins during flagellar regeneration in Chlamydomonas. *J. Cell Biol.* **93**, 615-631.

Rosenbaum, J. L. and Carlson, K. (1969). Cilia regeneration in Tetrahymena and its inhibition by colchicine. *J. Cell Biol.* **40**, 415-425.

Rosenbaum, J. L. and Child, F. M. (1967). Flagellar regeneration in protozoan flagellates. *J. Cell Biol.* **34**, 345-364.

Rosenbaum, J. L. and Witman, G. B. (2002). Intraflagellar transport. *Nat. Rev. Mol. Cell Biol.* **3**, 813-825.

Rosenbaum, J. L., Moulder, J. E. and Ringo, D. L. (1969). Flagellar elongation and shortening in Chlamydomonas. The use of cycloheximide and colchicine to study the synthesis and assembly of flagellar proteins. *J. Cell Biol.* **41**, 600-619.

Satir, P., Mitchell, D. R. and Jékely, G. (2008). How did the cilium evolve? *Curr. Top. Dev. Biol.* **85**, 63-82.

Schroda, M. (2006). RNA silencing in Chlamydomonas: mechanisms and tools. *Curr. Genet.* **49**, 69-84.

Sharma, N., Bryant, J., Wloga, D., Donaldson, R., Davis, R. C., Jerka-Dziadosz, M. and Gaertig, J. (2007). Katanin regulates dynamics of microtubules and biogenesis of motile cilia. *J. Cell Biol.* **178**, 1065-1079.

Sharma, N., Kosan, Z. A., Stallworth, J. E., Berbari, N. F. and Yoder, B. K. (2011). Soluble levels of cytosolic tubulin regulate ciliary length control. *Mol. Biol. Cell* **22**, 806-816.

Shimogawara, K., Fujiwara, S., Grossman, A. and Usuda, H. (1998). High-efficiency transformation of Chlamydomonas reinhardtii by electroporation. *Genetics* **148**, 1821-1828.

Silflow, C. D., Chisholm, R. L., Conner, T. W. and Ranum, L. P. (1985). The two alpha-tubulin genes of Chlamydomonas reinhardi code for slightly different proteins. *Mol. Cell. Biol.* **5**, 2389-2398.

Sizova, I., Fuhrmann, M. and Hegemann, P. (2001). A Streptomyces rimosus aphVIII gene coding for a new type phosphotransferase provides stable antibiotic resistance to Chlamydomonas reinhardtii. *Gene* **277**, 221-229.

Song, L. and Dentler, W. L. (2001). Flagellar protein dynamics in Chlamydomonas. *J. Biol. Chem.* **276**, 29754-29763.

Stephens, R. E. (1977). Differential protein synthesis and utilization during cilia formation in sea urchin embryos. *Dev. Biol.* **61**, 311-329.

Walczak, C. E., Gan, E. C., Desai, A., Mitchison, T. J. and Kline-Smith, S. L. (2002). The microtubule-destabilizing kinesin XKCM1 is required for chromosome positioning during spindle assembly. *Curr. Biol.* **12**, 1885-1889.

Weeks, D. P. and Collis, P. S. (1976). Induction of microtubule protein synthesis in Chlamydomonas reinhardi during flagellar regeneration. *Cell* **9**, 15-27.

Wilson, N. F. and Lefebvre, P. A. (2004). Regulation of flagellar assembly by glycogen synthase kinase 3 in Chlamydomonas reinhardtii. *Eukaryot. Cell* **3**, 1307-1319.

Youngblom, J., Schloss, J. A. and Silflow, C. D. (1984). The two beta-tubulin genes of Chlamydomonas reinhardtii code for identical proteins. *Mol. Cell. Biol.* **4**, 2686-2696.